

# METROLOGICAL CHARACTERIZATION OF A CYCLE-ERGOMETER

Bocciolone Marco, Comolli Lorenzo

*Department of Mechanical Engineering, Politecnico di Milano, Via La Masa 34, 20156 Milano, Italy*

Molteni Franco

*Valduce Hospital, Villa Beretta Rehabilitation Center, Via N.Sauro 17, Costamasnaga (LC), Italy*

**Keywords:** Cycle-ergometer, wireless data transmission, mechanical measurements, data analysis, rehabilitation.

**Abstract:** A cycle-ergometer has been instrumented with suitable strain gauges to obtain metrological qualified measurements of the left and right leg torque. A wireless device has been used to transmit in real-time the gathered signals to the acquisition PC. Advantages are to give to doctors and physiotherapists a diagnostic tool, to analyze the cycling pattern of the patients and to monitor the improvements during rehabilitation. The real-time measures are also suitable input data for the Functional Electrical Stimulation (FES). All the analysis was conducted with a particular attention to spinal cord injured patients, who are characterized by highly asymmetric cycling: yet, this measurement setup, by independent measurement of right and left torques, can be used successfully also in this particular situation. An explanation of the measuring principles and a set of first results are given, that show the potentiality of the setup.

## 1 INTRODUCTION

The present work is aimed at the metrological characterization of a commercial cycle-ergometer, used in clinical and private field, for the rehabilitation of people who need a motor therapy. The device shows on a display the mean value of clinical parameters: subject's motor power, angular velocity, energy, right and left leg unbalance. Those values are computed using electrical quantities from the motor and the unbalance supposes that one of the legs is not opposing a relevant resistance to the motion. These average measurements proved to be quite accurate on healthy subjects, but problems could arise in the unbalance measurement especially with strongly asymmetric spinal cord injured patients. Indeed, in the standard device, the unbalance is computed by splitting the revolution in half; but in asymmetric patients one of the legs typically has a bigger resistance during flexure respect to extension (e.g. due to spasticity, contracture or joint limitation), that could lead to systematic errors. The proposed measurement of independent left and right torques would solve the problem. An introduction to the devices can be found in (Comolli et al., 2005).

Moreover the average data on the display are not saved. To give specialists a better idea of the rehabilitation of a patient, a recording and tracking of the data should be done, together with an *a-posteriori* appropriate data analysis to quantify the improvements of the treatment.

Another advantage of having a real time measurement setup is to provide a proper input to a Functional Electrical Stimulation (FES) system such as that in (Ferrante et al., 2005 and 2006).

## 2 CYCLE-ERGOMETER INSTRUMENTATION

The employed cycle-ergometer provides the mean value of the above parameters by using measurement techniques and data processing that, in particular working situations (typically asymmetries), could give unreliable information. In order to overcome those limitations and to have instantaneous information, an independent measurement system has been designed and developed, using mechanical

sensors. Such system provides the following quantities:

- **bending moments ( $M_b$ ) and radial forces ( $F_r$ )** of right and left cranks: through two Wheatstone full-bridges each made up of electrical resistance strain gauges;
- **angular crank position ( $\theta$ )**: through optical encoders (Gföhler et al., 2001; Mimmi, Pennacchi & Frosini, 2004) drawn with white and black sectors on the main wheel (see Appendix for additional solutions).

Strain gauges are sensors suitable for superficial strain measurements. To measure the bending moments and radial forces, the gauges must be positioned in the appropriate position and direction on the crank, and must be connected on a Wheatstone full-bridge electrical circuit (made of 4 strain gauges) so that the voltage output is made proportional only to the selected quantity. An analysis of the strains present on the crank, subject to a generic force on the pedal axis, and the application of the basic laws of the theory of elasticity, will lead to the conclusion that for the measurement of the bending moment the sensors must be positioned near the crank axis, where the strain is larger, two on the upper and two on the lower surfaces, with the sensing direction along the crank longer dimension. The radial forces can be measured with two opposite strain gauges with the sensing direction along the crank longer dimension in a position corresponding to the smaller section; but to complete the Wheatstone bridge, two more strain gauges are necessary and they will be positioned transverse to the former so that they will sense transverse strain.

The positions on the Wheatstone bridge of each group of 4 strain gauges are selected such that compensation of radial forces and bending moments are achieved respectively in the bridges apt to measure the bending moment and radial force. Moreover temperature compensation is achieved automatically by means of auto-compensated strain gauges for the crank material (steel) and also thanks to the full-bridge properties. In this specific application, the locations of strain gauges are shown in Figure 4, with the numbers corresponding to specific positions on the Wheatstone bridge, according to the conventions of Figure 12. A detailed description of the applied methods can be found in Doebelin, 2003, Hoffmann, 1989 and Cigada, Comolli and Manzoni, 2006.

The strain gauge bridges are conditioned through a four-channel wireless device, which allows to transmit the signal from the rotating shaft to the acquisition system. This solution was selected after also considering slip rings and capacitive coupling (Mimmi et al., 2004), both of which required too much additional space.

The selected components are very compact: the wireless device is mounted on the left side crank inside a metal protection box (Figure 1); the connections between the sensors located on the right and left side of the device are realized by means of a multi-core cable passing through the crank axis (Figure 2). The power supply is given by an internal hi-capacity rechargeable battery that provides up to 9 h working time. The transmitted data are then converted in analog signals and acquired with a traditional DAQ board.



Figure 1: The strain gauge wireless acquisition device is inside the blue box, mounted on the left crank.



Figure 2: The right crank with the strain gauges wires passes through the axis to be connected to the wireless device that is on the other crank.

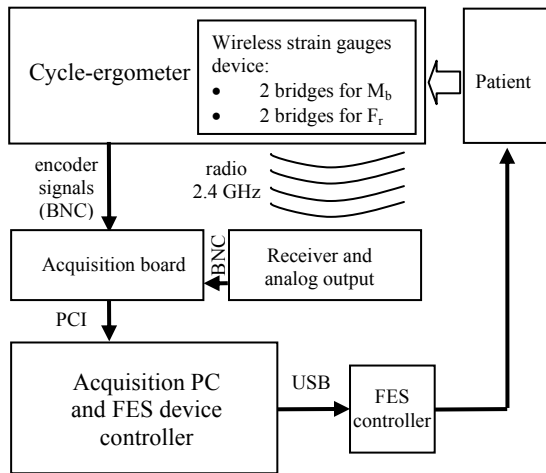


Figure 3: Scheme of the measuring chain and feedback on the patient.

### 3 MEASURED QUANTITIES

The measurement setup was designed and developed in order to identify the torque  $T$  as a combination of the bending moment  $M_b$  and the radial force  $F_r$  (Figure 4).

Known all the dimensions of the crank, the torques  $T$  are given by:

$$\begin{aligned} T_R &= M_{b,R} \frac{b}{d} - F_{r,R} \frac{e(b-d)}{d} \\ T_L &= M_{b,L} \frac{b}{d} - F_{r,L} \frac{e(b-d)}{d} \end{aligned} \quad (1)$$

where  $b$ ,  $d$ ,  $e$  are the dimensions shown in Figure 4, and  $L$  and  $R$  pedes are respectively referred as the left and right leg.

The instantaneous total power  $P_{tot}$  can be computed, known the angular velocity  $\dot{\theta}$  measured by the encoder, as:

$$P_{tot} = (T_R + T_L) \cdot \dot{\theta} \quad (2)$$

Moreover the mean energy per revolution can be computed as:

$$E_{m,tot} = \int_{t_1}^{t_2} P(t) \cdot dt \quad (3)$$

where  $t$  is the time and  $t_1$  and  $t_2$  are the instants of start and end of a revolution.

The unbalance  $U$ , a very significant quantity for asymmetric patients, can be computed as:

$$U = \frac{E_{m,R} - E_{m,L}}{E_{m,tot}} \quad (4)$$

where a positive value of  $U$  mean an unbalance toward the right leg that is more powerful.

Another useful quantity is the jerk  $J$ , i.e. the rate of change of angular acceleration, which shows the fluidity of the motion (Schot, 1978 and Teulings et al., 1997). Absolute jerk is defined as the third derivative of angular position, while a more interesting parameter is  $J_{std}$ , the standard deviation of jerk computed per revolution:

$$\begin{aligned} J &= \ddot{\theta} \\ J_{std} &= \sqrt{\frac{1}{(t_2 - t_1)} \int_{t_1}^{t_2} (J - \bar{J})^2 dt} \end{aligned} \quad (5)$$

where  $\bar{J}$  is the mean jerk in one revolution.

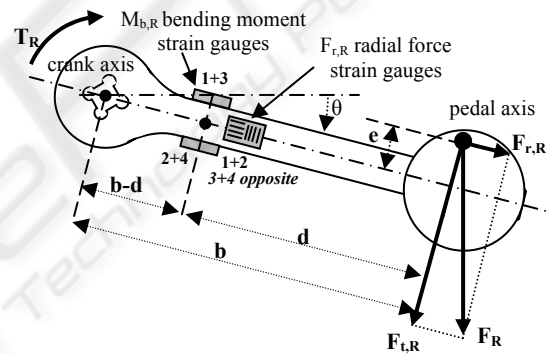


Figure 4: Scheme of the positioning of strain gauges on the right crank. For the strain gauges numbering conventions, see Figure 12.

### 4 FIRST RESULTS

The identification of the motor strategy of a patient and the comparison with healthy subjects (or with the same patient before rehabilitation) is fundamental to diagnose a pathology and verify the progress. The modified cycle-ergometer gives to the doctors and physiotherapist many information: in the following some examples.

Figure 5 shows a spinal cord injured patient cycling with the help of FES. Such a patient can cycle also without FES because the cycle-ergometer is motorized and maintains a minimum speed. But the muscles of the insane leg would never make any work and may loose mass. FES permits also the use

of those muscles and therefore let them grow in size, even if the patient cannot control them.



Figure 5: A spinal cord injured patient cycling with the help of FES.

Figures 6-9 show an example of data that can be retrieved from the measuring system. A healthy subject was asked to cycle in different conditions, such as active (time 0-15 s), passive (15-40 s), active (40-58 s, various powers), only right leg (58-68 s) and only left leg (68-82 s).

Figure 6 shows the angular position and the three derivatives that are necessary to compute all the subsequent quantities.

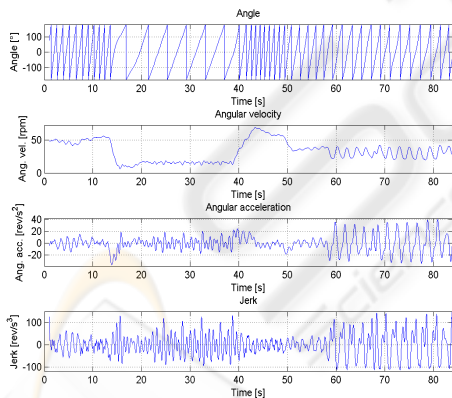


Figure 6: Angle and derivatives from cycling data of a healthy subject in different operating conditions.

In Figure 7 the standard deviation of jerk per revolution was computed; this quantity has relevant information: particularly the higher jerk is obtained when only one leg is used, this is due to the higher speed variations. Values up to 20  $\text{rev/s}^3$  are normal for healthy subjects during normal cycling with a high cycling resistance, while small values such as 2  $\text{rev/s}^3$  can be obtained with small resistance (not shown).

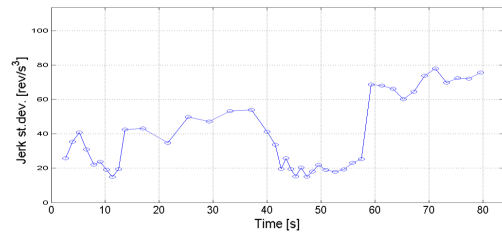


Figure 7: standard deviation of jerk per revolution: the biggest values are at right when only one leg was used.

The raw measurements would lead to instantaneous torque and power plots (not shown), with left, right and total components. Those information are interesting but highly difficult to analyze. A better solution has been found in re-phasing and averaging the torque values from some adjacent revolutions. Some examples will be shown ahead.

Average power and energy per revolution are shown in Figure 8, and give a good idea of the cycling conditions.

Figure 9 shows the percent unbalance and the total energy produced by the patient from the start of the test. Here also very small unbalance will build up and will be easily visible at the end of the test.

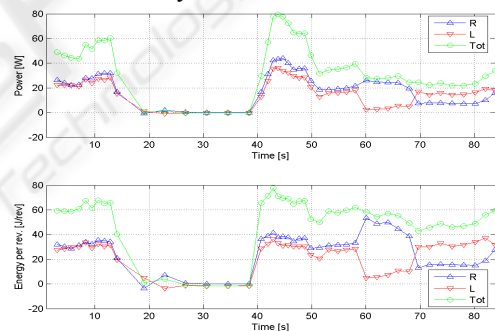


Figure 8: Average power and energy per revolution.

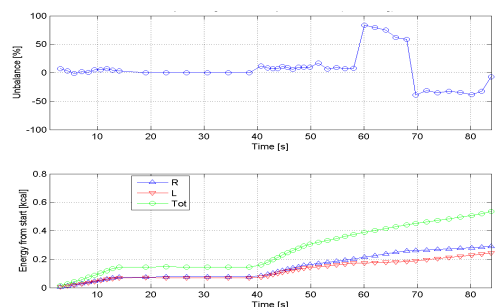


Figure 9: Unbalance and total energy from the start of the test.

A better way to evaluate the torque produced by the patient is to re-phase the torque signals and compute the median value in a number of revolutions. The median torque (along with percentiles) shows a



better waveform of the cycling and allows a better comparison between healthy and non healthy subjects and between the same patient before and after the rehabilitation. Figure 10 shows the torque from a healthy subject, while in Figure 11 the same subject was asked to use only the right leg. The zero crank angle is set at the maximum flexion of the left hip.

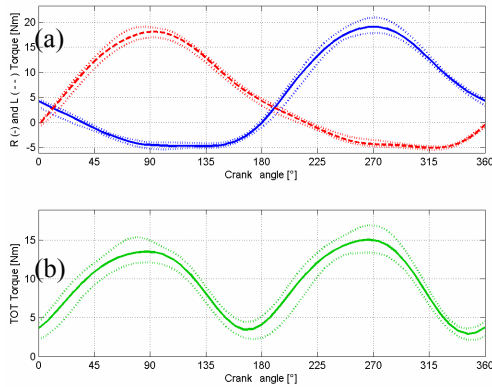


Figure 10: Median torque from a healthy subject actively cycling: (a) the left (dashed) and right (solid) components, (b) total torque that show nearly symmetric peaks. In dotted line the 5<sup>th</sup>-95<sup>th</sup> percentiles.

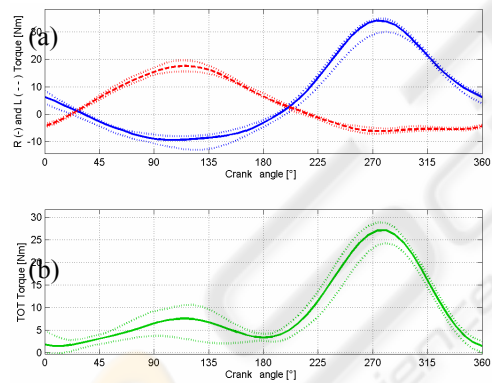


Figure 11: Same as the previous figure but related to a healthy subject, asked to cycle only with the right leg; the curves show highly asymmetric peaks.

The situation of a healthy subject asked to cycle only with the right leg simulates only one of the many possible cases of pathologic patients, where one of the legs is very weak but not completely passive. Indeed a healthy subject is unable to perform a true passive pedaling, as shown in Figure 11(a), where the left leg curve (dashed) is nearly flat in the angular range 270-360°, indicating that the weight of the leg is unconsciously partially compensated.

## 5 CONCLUSIONS

The paper deals with the design and the realization of a measurement system able to measure relevant quantities of the cycling, such as the torque (left, right and total), power, energy, unbalance and jerk.

The experimental tests involved both healthy subjects and spinal cord injured patients. Examples of the obtained measurements had been shown extensively in the figures. The results obtained up to now allowed the doctors and physiotherapists to have at their disposal additional and metrological qualified information, useful for diagnostic purposes and for checking the effects of the rehabilitation.

## ACKNOWLEDGEMENTS

This work was supported by the Fondazione Cariplo in the framework of the research program HINT@Lecco. Authors would like to acknowledge Mauro Rossini (Villa Beretta Rehabilitation Center) for his helpful discussion.

## REFERENCES

- Comolli, L., Cantatore, A., Zappa, E., Bocciolone, M., Molteni, F., 2005. HINT@LECCO project: metrological characterization of a cycle-ergometer., In *SIAMOC 05, 6th Congress of the Italian Society of Movement Analysis in Clinics*.
- Ferrante, S., Pedrocchi, A., Gioia, M., Ferrigno, G., Molteni, F., 2005. HINT@LECCO project: FES cycling optimization and first clinical experiments of on patients. In *SIAMOC 05, 6th Congress of the Italian Society of Movement Analysis in Clinics*.
- Ferrante, S., Pedrocchi, A., Ferrigno, G., Molteni, F., 2006. Experimental campaign of FES cycling on hemiplegics: first results. In *SIAMOC 06, 7th Congress of the Italian Society of Movement Analysis in Clinics*.
- Gföhler, M., Angeli, T., Eberharter, T., Lugner, P., Mayr, W., Hofer, C., 2001. Test Bed with Force-Measuring Crank for Static and Dynamic Investigations on Cycling by Means of Functional Electrical Stimulation. *IEEE Transactions On Neural Systems And Rehabilitation Engineering*, Vol. 9, No. 2, June 2001, pp. 169-180.
- Mimmi, G., Pennacchi, P., Frosini, L., 2004. Biomechanical Analysis of Pedalling for Rehabilitation Purposes: Experimental Results on Two Pathological Subjects and Comparison with Non-pathological Findings. *Computer Methods in Biomechanics and Biomedical Engineering*, Vol. 7, No. 6, Dec. 2004, pp. 229-345.

- Doebelin, E.O., 2003. *Measurement Systems*, McGraw-Hill, 5<sup>th</sup> edition.
- Hoffmann, K., 1989. *An introduction to measurements using strain gauges*, Hottinger Baldwin Messtechnik GmbH, 1<sup>st</sup> edition.
- Cigada, A., Comolli, L., Manzoni, S., 2006. *Estensimetria Elettrica*, CittàStudi Edizioni, 1<sup>st</sup> edition.
- Schot, S.H., 1978. Jerk: The time rate of change of acceleration, *American Journal of Physics*, Nov. 1978, Vol. 46, Iu. 11, pp. 1090-1094.
- Teulings, H.L., Contreras-Vidal, J.L., Stelmach, G.E., Adler, C.H., 1997. Parkinsonism Reduces Coordination of Fingers, Wrist and Arm in Fine Motor Control, *Experimental Neurology*, Vol 146, pp. 159-170.

## APPENDIX

For the crank angle measurement, a traditional encoder solution was chosen using a photo-reflective sensor coupled with a yet-present encoder drawn on the main cycle-ergometer wheel. Another two solutions have been also investigated.

The first solution was an inclinometer able to measure the bending of a beam with a small mass at the extreme, by means of strain gauges. The inclinometer has been positioned on the crank and have a nearly cosinusoidal output dependent on the angular position. The measured bending moment is proportional to the tangential acceleration  $a_t$  of the mass, which can be computed as:

$$a_t = g \cos \theta + \ddot{\theta} \rho \quad (6)$$

where  $g$  is the acceleration of gravity and  $\rho$  is the distance of the mass from the crank axis (see Figure 12). After the realization of an inclinometer with a small  $\rho$  value (Figure 13), the measurements showed that the angular acceleration term can be neglected and so the signal is actually a cosinusoid.

Another consideration is about the thickness of the beam that should not be too thin, this because a high natural frequency is desirable; but also not too thick because the bending must be measurable. The output signal was gathered with the same strain gauge wireless device used for moments and forces measurements, then it is filtered and analyzed to find the unknown angle. To solve the two solutions ambiguity of the arccosine function, the first derivative was considered: a negative value indicate that the solution is in the first or second quadrant.

Another studied solution takes advantage of a cam positioned on the crank axis (Figure 12); the distance of the cam to a fixed point on the cycle-ergometer was measured by means of a laser

triangulation transducer. The resulting signal is nearly cosinusoidal and can be analyzed in the same way of the inclinometer one. In fact the signal is of this kind:

$$r(\theta) = -e_c \cos \theta + \sqrt{R^2 - e_c^2} \sin \theta \quad (7)$$

where  $r$  is the distance from the crank axis of a point on the cam surface that cannot rotate with it,  $e_c$  is the cam eccentricity and  $R$  is the cam radius. With the proper selection of the dimensions, the cosinusoid approximation can give as low as  $\pm 5^\circ$  errors, as in the realized cam.

All the described measurement solutions were successfully used and proved to be of interest when no simpler alternatives are possible.

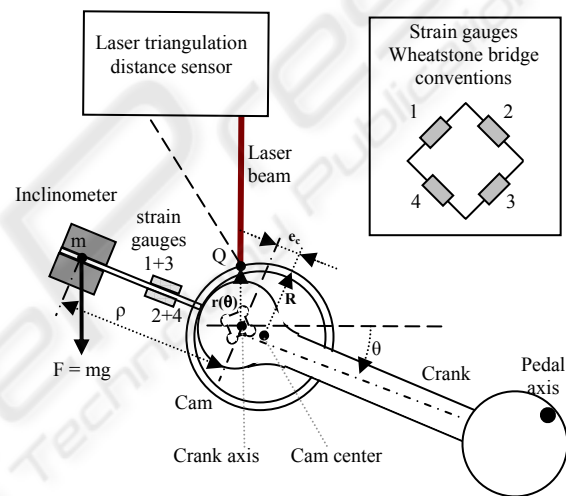


Figure 12: Scheme of the inclinometer and the cam mounted on the crank.



Figure 13: The adopted inclinometer.